On an Optimal Number of Time Steps for a Sequential Solution of an Elliptic-Hyperbolic System

Nikolay Andrianov

Schlumberger Research and Development,
5A Ogorodnaya Sloboda Per.,
101000 Moscow, Russia
Email: nandrianov@slb.com

Abstract

We consider a sequential approach for the solution of an elliptic-hyperbolic system of partial differential equations, which models a flow of two incompressible phases in porous media. The elliptic equation describes the pressure distribution in the domain, and the hyperbolic equation is the mass conservation equation for one of the phases. We propose to estimate an optimal number of the pressure updates using an analytical solution to a special 1D initial boundary value problem (IBVP) for the coupled system. We provide two procedures aimed at the estimation of an optimal set of time steps, and show that the resulting distribution of time steps yields better results than using equidistant time steps. We also show that the degree of coupling of the 1D IBVP can be quantitatively estimated using a normalized difference of the exact solution and its sequential approximation with a single time step.

Introduction

One well-established method for numerical solution of the equations for the multiphase flow in porous media is a sequential approach, which is based on a re-formulation of the mass conservation equations and Darcy's law (see e.g. [1]). For the case of two incompressible phases with negligible capillary pressure and gravity effects (in this note we will restrict ourselves to this case), the re-formulated system of governing equations consists of the Laplace equation with variable coefficients for pressure, and the hyperbolic equation for the saturation of one of the phases.

In the sequential approach, the solution to the coupled elliptic-hyperbolic system is sought in two stages: Firstly, the elliptic pressure equation with frozen coefficients is solved, and the corresponding Darcy velocity field is found; secondly, the hyperbolic saturation transport equation is solved over a certain period of time using a frozen Darcy velocity field, so that the coefficients of the elliptic equation can be computed; and the process repeats. A specific choice of the discretization technique for the elliptic and

hyperbolic parts gives rise to a particular numerical method. Examples of the sequential method include IMPES-type methods [1, 2] and the method of streamlines [3].

One important question in the specification of the sequential approach is the choice of time instants at which the pressure field should be updated. In standard IMPES method, pressure is re-computed at each time step used for the solution to the hyperbolic transport equation, and the length of this common time step size is determined from CFL-like stability conditions [1, 2, 4]. In practice, this can require an excessive number of pressure updates for a simulation, which can make these methods computationally expensive. In the streamline method, one typically needs to estimate the number and length of pressure time steps before the actual computation. This decision is often based on engineering intuition.

It has been noted (see e.g. [5]) that pressure is smoother in time than the saturation, and that one may use larger time steps for pressure updates than for the saturation transport. In [6], the authors obtained the convergence rates of a finite element method when the pressure time step is chosen as a fixed multiple of the saturation time step. Different pressure and saturation time steps are intrinsic to the method of streamlines, see e.g. [6] for an overview. An *a posteriori* CFL-like estimate for the length of pressure time steps in the streamline method is proposed in [7]. Finally, there is a variety of heuristic estimates for the length of pressure time steps available in the literature, based on maximum allowed pressure and saturation change, convergence criteria, etc.–see e.g. [1, 2].

To the best of our knowledge, currently there are no theoretical *a priori* estimates on the length of pressure time steps. This note is intended to fill this gap to some extent. To this goal, we restrict ourselves to a simple physical setting: we consider a flow of two incompressible fluids with negligible capillary pressure and gravity effects, whereas the relative permeability curves are straight lines. Moreover, let the flow be 1D, either in Cartesian geometry, or for cylindrically or spherically symmetric cases. For the resulting elliptic-hyperbolic system, we consider the following initial boundary-value problem (IBVP): piecewise constant initial data for saturation, and constant pressure boundary conditions. The initial and boundary conditions are chosen in such a way that a single shock-type solution is admissible. Then, we formulate an ordinary differential equation (ODE) for the motion of the interface, separating left and right states of constant saturation, and find its exact analytical solution. This is done in a way similar to Muskat [8]. For the case of Cartesian geometry, we present the dimensionless form of the IBVP of interest, and show that its single shock-type solution can be completely determined by specifying three dimensionless parameters: the mobility ratio, the initial interface position, and a parameter related to the shape of the Buckley–Leverett flux function.

The sequential approach of the elliptic-hyperbolic system can be represented as a forward Euler integration of the ODE for the motion of the interface. Consequently, the sequential solution is a piecewise-linear approximation to the exact solution, and the vertices of this polygonal approximation correspond to the pressure time steps. We can estimate the accuracy of the polygonal approximation by e.g. considering its relative distance from the

exact solution. Based on this error estimate, we propose two algorithms for an optimal time step selection:

1. Given an approximation error per time step which we agree to tolerate, we find the time instants at which the pressure update should be performed.
2. Given a total number of pressure updates, we find the time instants at which the pressure updates should be performed. These are chosen by minimizing the approximation error using a nonlinear optimization method–the downhill simplex method, see e.g. [9].

Finally, we propose to quantitatively estimate the degree of coupling of the 1D elliptic-hyperbolic IBVP using a normalized difference of the exact solution and its sequential approximation with a single time step. The functional dependence of the decoupling error with respect to the three dimensionless determining parameters is illustrated on a sample test problem.

The rest of the paper is organized as follows. In Section 1, we formulate the mathematical problem of interest. In Section 2, we present the corresponding one-dimensional IBVP, integrate the ODE for the interface motion, and provide the admissibility conditions for the single shock-type solution, for Cartesian geometry and for cylindrically or spherically symmetric cases. For the case of Cartesian geometry, we present the dimensionless form of the IBVP and show that its solution is determined by three dimensionless parameters.
In Section 3 we describe two algorithms for an optimal time step selection for the IBVP of interest. In Section 4 we define the decoupling error of the elliptic-hyperbolic system and illustrate this concept on a sample test problem. We end up with conclusions and outlook in Section 5.

1. Problem formulation

In this work, we restrict ourselves to the case of two-phase incompressible fluids: oil and water. For the sake of simplicity we assume that both fluids differ in viscosity only and the rock is incompressible, and consider homogeneous media only, i.e. both porosity and permeability are constant. Furthermore, we neglect gravity and capillary forces.
The mass conservation equations are

$$\varphi \frac{\partial S_j}{\partial t} + \nabla \cdot \mathbf{u}_j = 0, \quad j = w, o \tag{1}$$

where the subscripts w and o stand for water and oil respectively, φ is porosity, S_j and $\mathbf{u}_j$ are the phase saturations and velocities, respectively. The system (1) is closed by Darcy's law

$$\mathbf{u}_j = -\mathbf{K}\lambda_j \nabla p, \tag{2}$$

where $\lambda_j = k_{rj} / \mu_j$ are the phase mobilities, $k_{rj} = k_{rj}(S_j)$ are the relative permeability functions, μ_j are viscosities, and $\mathbf{K} = \mathrm{diag}(K)$ is the permeability tensor. Throughout this work, we use the linear relative permeabilities only, i.e. $k_{rj}(S_j) = S_j$.

Taking into account the above-mentioned assumptions, a pressure-saturation formulation of the system (1)–(2) reads

$$\nabla \cdot \left(-\mathbf{K}\lambda \nabla p\right) = 0 \tag{3}$$

$$\varphi \frac{\partial S_w}{\partial t} + \mathbf{u} \cdot \nabla f_w = 0 \tag{4}$$

for $t \in [0, T_f]$, where $\lambda = \lambda_w + \lambda_o$ is the total mobility, $\mathbf{u} = \mathbf{u}_w + \mathbf{u}_o$ is the total velocity, and $f_w = \lambda_w / \lambda$ is the Buckley–Leverett flux function. The system (3)–(4) is a coupled elliptic-hyperbolic system for the variables (p, S_w): (3) is Laplace's equation with variable coefficients $\lambda = \lambda(S_w)$, and (4) is a transport equation with $u = u(S_w, \nabla p)$ from Darcy's law (2). The degree to which the equations (3) and (4) are coupled with each other is determined by how strong the dependence $\lambda = \lambda(S_w)$ is. In the limiting case when λ does not depend on S_w at all, the system (3)–(4) decouples.

The *sequential approach* to the solution of the system (3)–(4) consists in fixing a set of time steps $\Delta t_1, \ldots, \Delta t_N$ (called the *pressure time steps*) with $\Delta t_i = t_i - t_{i-1}$, $i = 1, \ldots, N$, $t_0 = 0$, $t_N = T_f$, and using the following procedure:

For $i = 0$ to $N - 1$ do

1. Find the pressure distribution $p(t_i)$ by solving the equation (3) with frozen coefficients $\lambda(S_w(t_i))$; Compute the corresponding velocity field $\mathbf{u}(t_i)$ from Darcy's law (2).
2. Find the saturation distribution $S_w(t_{i+1})$ by solving the equation (4) with frozen velocity field $\mathbf{u}(t_i)$.

A specific numerical method, based on this sequential approach, is determined by the discretization used for the pressure equation and for the saturation transport. In this work, we will mention only two numerical methods which fit into the sequential framework.

One well-known method is IMPES (see e.g. [1]), which employs an implicit finite-difference method for the solution of the pressure (3), and an explicit finite-difference method for the solution of the saturation equation (4). In this method, the time instants $t_1, \ldots, t_{N-1}$ are found from CFL-like stability conditions for the explicit method. This can require an excessive number of computationally expensive pressure updates, which often can make the overall method inefficient.

Another method of sequential solution is the streamline method, see e.g. [3]. Here, the pressure is typically solved with a finite-difference or finite-element method, and a set of streamlines is computed based on the corresponding Darcy velocity field. The 3D saturation equation (4) is re-formulated along the streamlines, thus becoming a 1D equation. Then, the saturations are updated for a set of streamlines, and mapped back to the 3D grid. There are two distinct sets of time steps in this method: time steps between the pressure updates, and time steps for the solution of saturation transport.

Since the pressure is generally smoother in time than the saturation, it is natural to choose larger time steps $\Delta t_1, \ldots, \Delta t_N$ than those dictated by stability conditions for the saturation transport. To the best of our knowledge, the majority of work devoted to the choice of pressure time steps is related to *a posteriori* estimates; see e.g. [2, 6, 7]. Available a priori estimates usually use heuristic arguments, like maximum allowed pressure and saturation change, convergence criteria, etc.–see e.g. [1, 2].

The goal of this paper is to provide an *a priori* estimate for an optimal choice of pressure time steps for the sequential solution of the system (3)–(4). Below we will give an exact definition of what we mean by "optimal" in this context.

The starting point in our considerations is the following. Imagine for the moment that we are able to solve both steps of the sequential approach analytically. Then the accuracy of the sequential approach (i.e., how well does it approximate the analytical solution of the coupled system (3)–(4)) is completely determined by the choice of pressure time steps. Next, observe that the number of pressure time steps needed to achieve a certain level of accuracy is directly related to the degree of coupling of the system (3)–(4). Indeed, in the limiting case when the equations (3) and (4) are completely decoupled, the sequential approach with just one pressure time step $\Delta t_1 = T_f - t_0$ gives the exact solution to the coupled system (3)–(4). When the coupling of equations (3) and (4) is weak, we will need to use several pressure time steps to achieve the same accuracy. Finally, in the extreme case when the system (3)–(4) is strongly coupled, we will need to update pressure with high frequency.

In subsequent section, we revise an analytical solution by Muskat [8] for a 1D restriction of the system (3)–(4). This will allow us to give a precise definition of terms "optimal choice of time steps" and "degree of coupling of the system" somewhat vaguely used above.

2. One-dimensional initial boundary-value problem

Consider the 1D formulation of the system (3)–(4) in case of Cartesian geometry, and for cylindrically and spherically symmetrical cases. We have

$$x^{-\alpha} \frac{d}{dx}\left(-K\lambda x^{\alpha} \frac{dp}{dx} \right) = 0 \tag{5}$$

$$\varphi \frac{\partial S}{\partial t} + u \frac{\partial f}{\partial x} = 0, \tag{6}$$

where in (6) we have dropped the subscript w for brevity. In (5), $\alpha = 0$ corresponds to the Cartesian geometry, $\alpha = 1$ and $\alpha = 2$ correspond to cylindrically and spherically symmetrical cases respectively, with x being the radial distance. Let us use the following initial and boundary conditions for the system (5)–(6):

$$S(x,t) = \begin{cases} S_l, & a \le x < h_0 \\ S_r, & h_0 < x \le b, \end{cases} \qquad p(a,t) = p_l, \quad p(b,t) = p_r. \tag{7}$$

Here $0 < a < b$, $h_0 \in (a,b)$ is fixed, and the subscripts l and r refer to left and right states, respectively. The initial data in (7) correspond to a sharp interface located at $x = h_0$ and separating the left and right states with constant (water) saturations S_l and S_r, respectively.

Physically, the solution to the initial boundary-value problem (IBVP) (5)–(7) describes an evolution of the interface, originally located at h_0, under the action of the pressure difference $p_r - p_l \neq 0$. In what follows, we will seek a solution to the IBVP (5)–(7) which actually *preserves* the discontinuity in $S = S(x,t)$, i.e. the solution has a form of a single jump (or shock), connecting S_l to S_r, see Figure 1. We will postpone the discussion on the admissibility of such a solution until the end of the subsequent section.

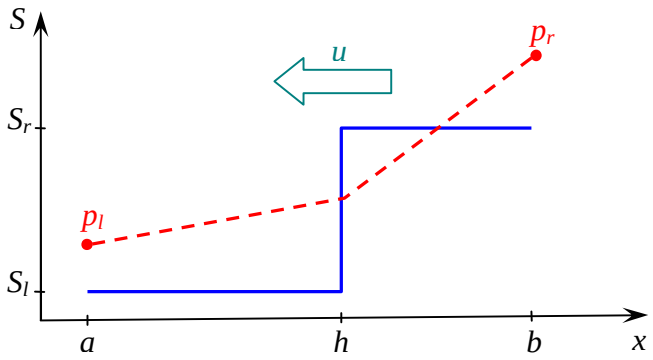

Figure 1. A snapshot of a single shock-type solution, propagating in the domain under the action of pressure difference.

2.1. A single shock-type solution

Assume for the moment that for all $t \in [0, T_f]$ the solution to the IBVP (5)–(7) for the saturation has the form

$$S(x,t) = \begin{cases} S_l, & a \le x < h \\ S_r, & h < x \le b, \end{cases} \tag{8}$$

where $h = h(t)$ is the current position of the interface. Then, the coefficient $\lambda = \lambda(x,t)$ in the pressure equation (5) becomes discontinuous,

$$\lambda(x,t) = \begin{cases} \lambda_l, & a \le x < h \\ \lambda_r, & h < x \le b, \end{cases} \tag{9}$$

where we have introduced $\lambda_{l,r} = \lambda(S_{l,r})$. Since by the assumption the interface at $h = h(t)$ separates constant values S_l and S_r, the values $\lambda_{l,r}$ are constant as well.

For the integration of the pressure equation (5) we need to augment the boundary conditions in (7) by the following compatibility conditions across the interface:

$$p(h_-) = p(h_+), \qquad \lambda_l \left.\frac{dp}{dx}\right|_{h_-} = \lambda_r \left.\frac{dp}{dx}\right|_{h_+}, \tag{10}$$

where $h_\pm$ refer to the states to the right and to the left of the interface, respectively. The equations (10) express the conditions that the pressure and Darcy's velocity should be continuous across the interface. Now the solution to the pressure equation (5) reads

$$p = \begin{cases} \lambda_r \dfrac{p_r - p_l}{\lambda_r (h^{-\alpha+1} - a^{-\alpha+1}) - \lambda_l (h^{-\alpha+1} - b^{-\alpha+1})} \left(x^{-\alpha+1} - a^{-\alpha+1}\right) + p_l, & a < x < h \\ \lambda_l \dfrac{p_r - p_l}{\lambda_r (h^{-\alpha+1} - a^{-\alpha+1}) - \lambda_l (h^{-\alpha+1} - b^{-\alpha+1})} \left(x^{-\alpha+1} - b^{-\alpha+1}\right) + p_r, & h < x < b \end{cases} \tag{11}$$

for $\alpha \neq 1$, and

$$p = \begin{cases} \lambda_r \dfrac{p_r - p_l}{\lambda_r (\ln h - \ln a) - \lambda_l (\ln h - \ln b)} \left(\ln x - \ln a\right) + p_l, & a < x < h \\ \lambda_l \dfrac{p_r - p_l}{\lambda_r (\ln h - \ln a) - \lambda_l (\ln h - \ln b)} \left(\ln x - \ln b\right) + p_r, & h < x < b \end{cases} \tag{12}$$

for $\alpha = 1$. The corresponding Darcy's velocity is

$$u = -K\lambda_l \lambda_r \frac{p_r - p_l}{\lambda_r (h^{-\alpha+1} - a^{-\alpha+1}) - \lambda_l (h^{-\alpha+1} - b^{-\alpha+1})} (-\alpha + 1)\, x^{-\alpha} \tag{13}$$

for $\alpha \neq 1$, and

$$u = -K\lambda_l \lambda_r \frac{p_r - p_l}{\lambda_r (\ln h - \ln a) - \lambda_l (\ln h - \ln b)} \frac{1}{x} \tag{14}$$

for $\alpha = 1$.

The speed of propagation of the interface located at $h = h(t)$ is given by the Rankine–Hugoniot jump condition (see e.g. [10]):

$$\frac{dh}{dt} = \frac{u(h)}{\varphi} \frac{f(S_r) - f(S_l)}{S_r - S_l}, \tag{15}$$

where we have used that the total Darcy velocity $u = u_w + u_o$ is continuous across the interface, cf. (13) and (14). Note that the interface speed dh/dt does not necessarily coincide with phase velocities u_w and u_o. Consequently, our results on the interface motion (see below) will slightly differ from the corresponding results of Muskat [8], who has used an assumption that an interface is always composed of the same fluid particles.

With the initial data

$$h(t = 0) = h_0 \tag{16}$$

we can easily integrate the autonomous ordinary differential equation (ODE) (15), using the expression (13) or (14) for Darcy's velocity. We have

$$t = \frac{1}{(-\alpha + 1)D} \left(\frac{M - 1}{2} \left(h^2 - h_0^2\right) + \frac{1}{\alpha + 1} \left(b^{-\alpha+1} - Ma^{-\alpha+1}\right)\left(h^{\alpha+1} - h_0^{\alpha+1}\right) \right) \tag{17}$$

for $\alpha \neq 1$, and

$$t = \frac{1}{D}\left(\frac{M-1}{2}\left(h^2 \ln h - h_0^2 \ln h_0 - \frac{1}{2}\left(h^2 - h_0^2\right)\right) + \frac{1}{2}\left(\ln b - M \ln a\right)\left(h^2 - h_0^2\right)\right) \tag{18}$$

for $\alpha = 1$. Here $M = \lambda_r / \lambda_l$ is the *mobility ratio*, and

$$D = -\frac{K}{\varphi}\lambda_r (p_r - p_l)\frac{f(S_r) - f(S_l)}{S_r - S_l}. \tag{19}$$

For the Cartesian case ($\alpha = 0$) the equation (17) can be easily resolved to obtain the dependency of the form $h \propto \sqrt{t}$. For the cylindrically symmetrical case ($\alpha = 1$) the equation (18) cannot be resolved in the class of elementary functions with respect to h. For the spherically symmetrical case ($\alpha = 2$) from equation (17) we can obtain a functional dependence $h = h(t)$ using Cardano's formula.

The solution to the ODE (15) with the initial data (16) is equivalent to a single shock-type solution to the coupled elliptic-hyperbolic system (5), (6) with the initial data (7). Knowing the interface position $h = h(t)$ from (17) or (18), the single shock-type solution to the IBVP (5)–(7) is given by (8) and either (11) or (12), depending on the value of α.

Now let us investigate on the admissibility of the single shock-type solution, determined by the relations (17) or (18). By assumptions on the shape of relative permeability curves, the flux function has the form

$$f(S) = \frac{\mu_o S}{\mu_o S + \mu_w (1 - S)}. \tag{20}$$

This is either a strictly convex, or a strictly concave function depending on the sign of the viscosity difference $\mu_o - \mu_w$. Therefore, we can use the Lax admissibility criterion (see e.g. [10]):

$$\frac{u(h_-)}{\varphi}\frac{df}{dS}\bigg|_{S(h_-)} \geq \frac{dh}{dt} \geq \frac{u(h_+)}{\varphi}\frac{df}{dS}\bigg|_{S(h_+)}, \tag{21}$$

where $h_\pm$ refer to the states to the right and to the left of the interface, respectively. Since u is continuous across the interface, we have $u(h_-) = u(h_+) = u(h)$. By assumption, the interface separates the states with constant values S_l and S_r, so $S(h_-) = S_l$ and $S(h_+) = S_r$. Using this in (21), we obtain the following admissibility conditions:

$$u(h)\frac{df}{dS}\bigg|_{S_l} \geq u(h)\frac{f(S_r) - f(S_l)}{S_r - S_l} \geq u(h)\frac{df}{dS}\bigg|_{S_r}. \tag{22}$$

Considering different cases of the double inequality (22), we establish that the interface $h = h(t)$ is admissible if and only if one of subsequent conditions holds:

$$p_l > p_r \quad (u > 0), \quad M > 1, \quad S_l < S_r \quad (v > 1) \tag{23}$$

$$p_l > p_r \quad (u > 0), \quad M > 1, \quad S_l > S_r \quad (v < 1) \tag{24}$$

$$p_l < p_r \quad (u < 0), \quad M < 1, \quad S_l > S_r \quad (v > 1) \tag{25}$$

$$p_l < p_r \quad (u < 0), \quad M < 1, \quad S_l < S_r \quad (v < 1). \tag{26}$$

Here we have introduced the viscosity ratio $\nu = \mu_o / \mu_w$. Admissibility conditions (23)–(26) can be summarized as follows: For an admissible interface the mobility ahead of the interface is to be greater than the mobility behind the front. This a well-known interface stability criterion, related to viscous fingering, see e.g. [11].

2.2. Dimensionless formulation

In subsequent sections it will be convenient to use dimensionless form of the IBVP (5)–(7). From here on we will restrict ourselves to the case of Cartesian geometry $\alpha = 0$ only; the cylindrically and spherically symmetrical cases can be treated analogously.

Let us undimensionalize the IBVP (5)–(7) with the scaling

$$\tilde{x} = \frac{x-a}{b-a}, \quad \tilde{p} = \frac{p-p_l}{|p_r - p_l|}, \quad \tilde{\lambda} = \frac{\lambda}{\lambda_l}, \quad \tilde{K} = \frac{K}{K_{\text{ref}}}, \tag{27}$$

where K_{ref} is a constant reference absolute permeability, which will be specified later. The choice for the dimensionless pressure $\tilde{p}$ implies that the pressure gradients (and thus the Darcy velocities) for both dimensional and dimensionless cases have the same sign.

If one of the admissibility conditions (23)–(26) holds true, the dimensionless pressure satisfies the equation

$$\frac{d}{d\tilde{x}}\left(\tilde{\lambda}\frac{d\tilde{p}}{d\tilde{x}}\right) = 0, \qquad \tilde{x} \in [0,1], \qquad \tilde{\lambda} = \begin{cases} 1, & 0 \le \tilde{x} < \tilde{h} \\ M, & \tilde{h} < \tilde{x} \le 1 \end{cases}, \tag{28}$$

augmented with the compatibility conditions (10). The boundary conditions for the pressure equation (28) depend on the sign of the difference $p_r - p_l$. If we introduce the function $\text{sign}(\delta) = 1$ if $\delta > 0$ and $\text{sign}(\delta) = -1$ otherwise ($\delta \equiv p_r - p_l \neq 0$), the boundary conditions for (28) take the form $\tilde{p}(0) = 0$ and $\tilde{p}(1) = \text{sign}(p_r - p_l)$. Then, the solution to (28) is

$$\tilde{p} = \begin{cases} \text{sign}(p_r - p_l)\dfrac{M}{\tilde{h}(M-1)+1}\tilde{x}, & 0 \le \tilde{x} < \tilde{h} \\ \text{sign}(p_r - p_l)\left(\dfrac{M}{\tilde{h}(M-1)+1}(\tilde{x}-1)+1\right), & \tilde{h} < \tilde{x} \le 1. \end{cases} \tag{29}$$

Using the scaling (27) in 1D version of Darcy's law (2), we obtain the following expression for dimensionless Darcy's velocity

$$\tilde{u} = \frac{u}{u_{\text{ref}}}, \quad u_{\text{ref}} = K_{\text{ref}}\lambda_l\frac{|p_r - p_l|}{b-a}. \tag{30}$$

With this definition, the dimensionless form of Darcy's law is

$$\tilde{u} = -\tilde{K}\tilde{\lambda}\frac{d\tilde{p}}{d\tilde{x}}, \tag{31}$$

so that the dimensionless Darcy's velocity is

$$\tilde{u} = -\text{sign}(p_r - p_l)\frac{\tilde{K}M}{\tilde{h}(M-1)+1}. \tag{32}$$

Substituting the definitions (27) and (30) into the equation for the saturation transport (6), we obtain the following expression for the dimensionless transport equation:

$$\varphi\frac{\partial S}{\partial \tilde{t}} + \tilde{u}\frac{\partial f}{\partial \tilde{x}} = 0, \tag{33}$$

where we have introduced the dimensionless time

$$\tilde{t} = \frac{t}{T_{\text{ref}}}, \quad T_{\text{ref}} = \frac{b-a}{u_{\text{ref}}}. \tag{34}$$

A single shock solution to the elliptic-hyperbolic system of dimensionless equations (28), (33) satisfies the Rankine–Hugoniot condition

$$\frac{d\tilde{h}}{d\tilde{t}} = \frac{\tilde{u}(\tilde{h})}{\varphi}\frac{f(S_r)-f(S_l)}{S_r - S_l}, \qquad \tilde{h}(\tilde{t}_0 = 0) = \tilde{h}_0. \tag{35}$$

This can be rewritten as

$$\frac{d\tilde{h}}{d\tilde{t}} = \frac{\tilde{D}M}{\tilde{h}(M-1)+1}, \qquad \tilde{h}(\tilde{t}_0 = 0) = \tilde{h}_0, \tag{36}$$

where

$$\tilde{D} = -\text{sign}(p_r - p_l)\frac{\tilde{K}}{\varphi}\frac{f(S_r)-f(S_l)}{S_r - S_l}.$$

The ODE (36) can be integrated to give

$$\tilde{h} = \frac{1}{M-1}\left(\sqrt{2\tilde{D}M(M-1)\tilde{t} + \left((M-1)\tilde{h}_0 + 1\right)^2} - 1\right), \quad M \neq 1. \tag{37}$$

Here $\tilde{t} \in [0, \tilde{T}_f]$, and the dimensionless final time $\tilde{T}_f = T_f / T_{\text{ref}}$ is chosen from the condition that the interface $\tilde{h} = \tilde{h}(\tilde{T}_f)$ remains in the domain [0,1]. Knowing the interface position $\tilde{h} = \tilde{h}(\tilde{t})$ from (37), we can obtain the saturations and pressure distribution for all $\tilde{x} \in [0,1]$ analogously to the dimensional case above.

The solution (37) is valid for non-degenerate cases $M \neq 1$ only. In the limiting case $M = 1$ the system (28), (33) decouples. Indeed, using $M = 1$ in (29) we see that the solution to the pressure equation (28) does not depend on the instantaneous position of the interface $\tilde{h} = \tilde{h}(\tilde{t})$. Then, a single shock solution to the to the transport equation (33) is a straight line

$$\tilde{h} = \tilde{h}_0 + \tilde{D}\,\tilde{t}\,. \tag{38}$$

The number of dimensionless parameters, determining the solution to the equation (37), can be reduced by using an appropriate definition of the reference absolute permeability K_{ref}, see (27). Namely, if we define

$$K_{\text{ref}} = \frac{K}{\varphi}, \tag{39}$$

so that the fraction $\tilde{K}/\varphi = 1$, then we have

$$\tilde{D} = -\text{sign}(p_r - p_l)\frac{f(S_r) - f(S_l)}{S_r - S_l}. \tag{40}$$

Thus, the complete solution to the system of equations (28), (33) is fully determined by three dimensionless parameters: the mobility ratio M, the initial interface position $\tilde{h}_0$, and the parameter $\tilde{D}$, related to the shape of the Buckley–Leverett flux function f.

3. Optimal time step selection for the one-dimensional case

The sequential approach for solving the dimensionless ODE (35) is precisely the forward Euler method

$$\tilde{h}_{i+1} = \tilde{h}_i + \Delta\tilde{t}_i \frac{\tilde{u}(\tilde{h}_i)}{\varphi}\frac{f(S_r) - f(S_l)}{S_r - S_l}, \quad i = 1, \ldots, N, \tag{41}$$

where $\tilde{h}_i = \tilde{h}_i(\tilde{x}) = \tilde{h}_i(\tilde{t}_i, \tilde{x})$ and $\Delta\tilde{t}_i = \tilde{t}_i - \tilde{t}_{i-1}$ are the pressure time steps. Indeed, in this 1D case the solution to the saturation transport reduces to an update of the interface position. As we have seen in Section 2, from the current interface position we can obtain the complete solution of the dimensionless equations (28), (33) and thus to the dimensional IBVP (5)–(7).

The Euler method (41) provides a first order approximation to the exact solution of the ODE (35). Therefore, the same is true also for the sequential approach for the solution of the IBVP (5)–(7).

Since the amount of work involved in the Euler method (41) is proportional to the number of individual steps, one will attempt to choose the step sizes $\Delta\tilde{t}_i$ as large as possible. On the other hand, they must not be chosen too large if one wants to keep the discretization error small. Another constraint on the step sizes $\Delta\tilde{t}_i$ can come from stability conditions, which is specifically the case for stiff ODEs. For the test cases presented below, we did not experience any stability problems with the Euler method (41), and therefore did not investigate on its stability properties for the particular case of the IBVP (28), (33). Instead, we concentrate on a choice of a minimal set of time steps $\Delta\tilde{t}_i$ which result in certain accuracy of the Euler method (41).

Graphically, the approximation (41) to the exact solution of the ODE (35) can be represented as a piecewise-linear function, which consists of linear segments $\left[(\tilde{t}_i, \tilde{h}_i); (\tilde{t}_{i+1}, \tilde{h}_{i+1})\right]$ with slopes $\frac{\tilde{u}(\tilde{h}_i)}{\varphi}\frac{f(S_r) - f(S_l)}{S_r - S_l}$, i.e. the segments are aligned with the

integral curves of the ODE (35). As a measure of accuracy of the Euler method (41) at time instant $\tilde{t}_i$ we will use the difference

$$d(\tilde{t}_i) := \frac{\left|\tilde{h}(\tilde{t}_i) - \tilde{h}_i\right|}{d_{\max}} \cdot 100\%, \tag{42}$$

where $\tilde{h}(\tilde{t}_i)$ is the exact solution to the ODE (35) at time $\tilde{t}_i$, the values $\tilde{h}_i$ are furnished by the Euler method (41), and $d_{\max}$ is the maximal difference between the sequential and exact solutions. This difference is the worst case error which is achieved at final time $\tilde{t}_N = T_f / T_{\text{ref}}$ when the sequential method uses just one time step:

$$d_{\max} = \left|\tilde{h}(\tilde{t}_N) - \left(\tilde{h}_0 + (\tilde{t}_N - \tilde{t}_0)\frac{\tilde{u}(\tilde{h}_0)}{\varphi}\frac{f(S_r) - f(S_l)}{S_r - S_l}\right)\right|. \tag{43}$$

It is illuminating to see how the different number of time steps affects the quality of the sequential solution (41). For instance, let us consider the following problem.

Problem 1. Interface motion in Cartesian geometry. In the domain with $a = 1\,\text{m}$ and $b = 100\,\text{m}$, an initial interface at $h_0 = 2\,\text{m}$ separates the states with water saturation $S_l = 0.1$ to the left and $S_r = 0.9$ to the right. The rock has porosity $\varphi = 0.3$ and absolute permeability $K = 500\,\text{mD}$, and the fluids have viscosities $\mu_w = 10\,\text{cP}$ and $\mu_o = 50\,\text{cP}$, respectively. The interface moves right under the action of the pressure gradient: $p_l = 200\,\text{bar}$, $p_r = 150\,\text{bar}$. Since the flow satisfies the admissibility conditions (23), the sharp interface remains in the solution, and its position can be determined from (37).

The dimensionless formulation of this problem consists in specifying the parameters $M = 3.28$, $\tilde{h}_0 = 0.01$, and $\tilde{D} = 0.77$. In Figure 2 we compare the exact solution to Problem 1 with two sequential solutions (41): The one using three equidistant time steps, and another using just one time step. Obviously the single step solution (a single linear segment) yields the worst approximation to the exact solution: the interface position at final time is overestimated by factor 1.8. The sequential solution with 3 equidistant time steps yields significantly better accuracy of 18.5% at final time.

This behaviour can be easily understood from the ODE for the interface motion (36). Observe that the Darcy velocity (32) and thus the derivative $d\tilde{h}/d\tilde{t}$ takes maximal values for small $\tilde{h}$. Thus, the single step solution, i.e. the straight line with the slope $\dfrac{\tilde{D}}{\tilde{h}_0(M-1)+1}$, is steeper than the exact solution (37) with its gradually decreasing slope $\dfrac{\tilde{D}}{\tilde{h}(M-1)+1}$.

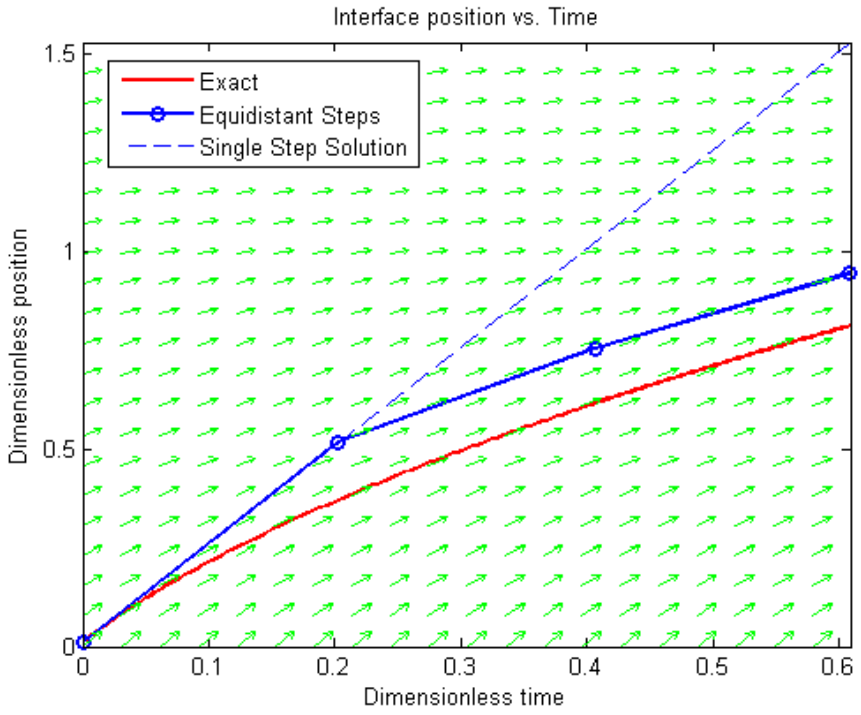

Figure 2. The analytical solution, the sequential solution using three equidistant time steps, and the single step solution for Problem 1. Arrows represent the slope field for the ODE (35). Segments of the sequential solution curve correspond to the pressure time steps.

From Figure 2 it is quite obvious that the accuracy of the Euler method (41) can be improved by considering variable size time steps. Indeed, in Figure 2 the curvature of the exact solution decreases in time, so one would get better accuracy using smaller time steps at the beginning of the simulation and larger steps at its end. In subsequent sections we will propose two procedures for an optimized variable time steps selection.

3.1. Fixed error time steps

A standard procedure used for the numerical solution of ODEs consists in determining the step sizes $\Delta\tilde{t}_i$ and their total number N from the condition that an error over this step does not exceed a prescribed tolerance, see e.g. [12]. Let us impose a condition that an error increase during a time step of the Euler method (41) is equal to a fixed level ε:

$$\frac{1}{d_{\max}}\left|\tilde{h}(\tilde{t}_i)-\left(\tilde{h}_{i-1}+(\tilde{t}_i-\tilde{t}_{i-1})\frac{\tilde{u}(\tilde{h}_{i-1})}{\varphi}\frac{f(S_r)-f(S_l)}{S_r-S_l}\right)\right|\cdot 100\% = \varepsilon\,. \qquad (44)$$

This is a nonlinear equation for the time instant $\tilde{t}_i$ which is solved with Newton's method for $\tilde{t}_i < \tilde{t}_N$. Typically, only several Newton iterations are sufficient to reach desired accuracy, so the overall procedure is fast. With the resulting set of N time steps

$\Delta\tilde{t}_i = \tilde{t}_i - \tilde{t}_{i-1}$ the accuracy of the Euler method (41) at final time $\tilde{t}_N$ is not greater than $N\varepsilon$.

Note that there is a possibility that the obtained set of N time steps does not necessarily deliver a minimal error at the final time $\tilde{t}_N$. The following procedure modifies the instants $\tilde{t}_i$ for given N, so that the final error is minimal among all sets of N time steps.

3.2. Final error minimization

Let us fix the total number of time steps N, and fix the initial and final time instants $\tilde{t}_0$ and $\tilde{t}_N$. We look for the set of time instants $\tilde{t}_i$, $i = 1,\ldots,N-1$ such that the error $d(\tilde{t}_N)$ at the final time $\tilde{t}_N$ is minimal, cf. (42). This is a multidimensional minimization problem with respect to the variables $\tilde{t}_1,\ldots,\tilde{t}_{N-1}$ under the obvious constraint $\tilde{t}_i < \tilde{t}_{i+1}$.

The Euler method (41) yields the following prediction for the interface position at the final time:

$$\tilde{h}_N = \tilde{h}_0 + \frac{1}{\varphi}\frac{f(S_r) - f(S_l)}{S_r - S_l}\sum_{i=1}^{N}\tilde{u}(\tilde{h}_{i-1})\,\Delta\tilde{t}_i\,. \tag{45}$$

Let us cast the right-hand side of (45) in form of a function

$$H(\tilde{t}_1,\tilde{t}_2,\ldots,\tilde{t}_{N-1}) = \tilde{h}_0 + \frac{1}{\varphi}\frac{f(S_r) - f(S_l)}{S_r - S_l}\sum_{i=1}^{N}\tilde{u}(\tilde{h}_{i-1})\,(\tilde{t}_i - \tilde{t}_{i-1})\,, \tag{46}$$

i.e., $H : R^{N-1} \to R$. We are interested in minimizing the error $d(\tilde{t}_N)$ at final time $\tilde{t}_N$:

$$\frac{1}{d_{\max}}\left|\tilde{h}(\tilde{t}_N) - H(\tilde{t}_1,\tilde{t}_2,\ldots,\tilde{t}_{N-1})\right|\cdot 100\% \mapsto \min\,. \tag{47}$$

Although the function $H = H(\tilde{t}_1,\tilde{t}_2,\ldots,\tilde{t}_{N-1})$ is given in analytical form (46), the expressions for its derivatives become extremely bulky for large N. For simplicity, we elect to solve the minimization problem (47) using a derivative-free Nelder–Mead simplex method [9].

It is illuminating to consider the dependence of the final error on the choice of the time steps for the case of Problem 1 (see page 12) using three time steps $\Delta\tilde{t}_i = \tilde{t}_i - \tilde{t}_{i-1}$, $i = 1,2,3$. This means that we have to choose two intermediate time instants $\tilde{t}_1$ and $\tilde{t}_2$ such that the error $d(\tilde{t}_3)$ will be minimal. The plot of the surface $d(\tilde{t}_3)$ vs. $\tilde{t}_1$ and $\tilde{t}_2$ is presented in Figure 3, where the set of admissible instants $\tilde{t}_1$ and $\tilde{t}_2$ is determined by the constraint $\tilde{t}_1 \le \tilde{t}_2$. Observe that the graph of the final error has three peaks: the first at $\tilde{t}_1 = \tilde{t}_2 = 0$, the second at $\tilde{t}_1 = 0$ and $\tilde{t}_2 = \tilde{t}_3$, and the third at $\tilde{t}_1 = \tilde{t}_2 = \tilde{t}_3$. All these cases correspond to a single step solution so that the error (42) is equal to 100%.

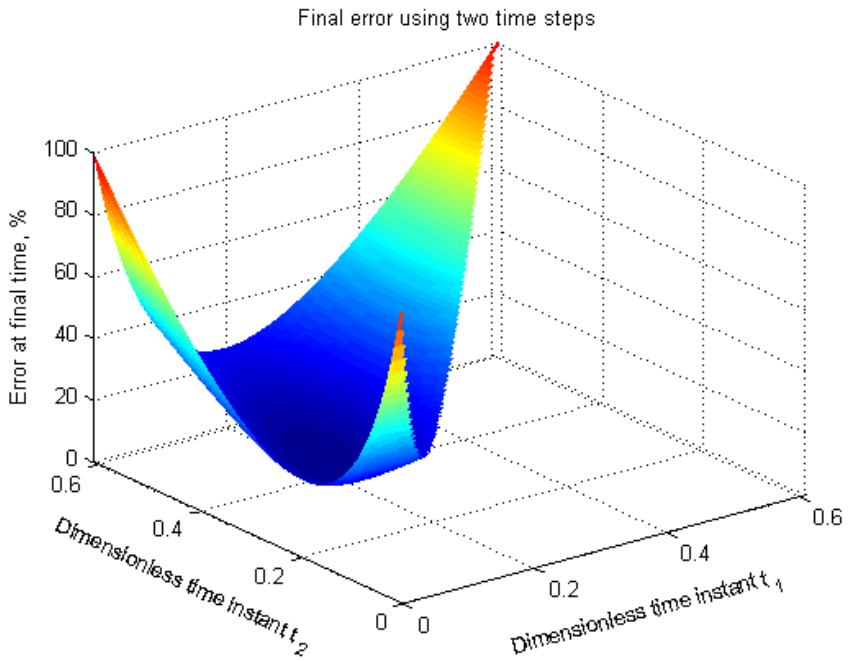

Figure 3. Final error in interface position for Problem 1 as a function of time instants $\tilde{t}_1$ and $\tilde{t}_2$.

The pair $(\tilde{t}_1, \tilde{t}_2)$, which yields the minimal value of the final error $d_{\min}$, is found numerically using the Nelder–Mead simplex method [9]. Since the graph in Figure 3 in a neighbourhood of its minimum value is relatively flat, the method requires several hundred iterations to converge. However, since each evaluation of the function (46) is computationally inexpensive, the overall algorithm is fast. From Figure 3 it becomes obvious that a certain level $d > d_{\min}$ corresponds to infinitely many pairs $(\tilde{t}_1, \tilde{t}_2)$. This means that the same final accuracy $d > d_{\min}$ of the Euler method (41) can be achieved with infinitely many different combinations of time steps $\Delta\tilde{t}_1$, $\Delta\tilde{t}_2$.

3.3. Comparison of the procedures

Let us apply the procedures from Section 3.1 and 3.2 for the solution of Problem 1 (page 12) in such a way that both procedures use only 3 time steps. This will allow us to see the advantages of these procedures over a simple choice of equidistant time steps, cf. Figure 2. The fixed error time steps procedure yields three steps if the error increase between two time steps is set to e.g. 10%, and for the final error minimization procedure we simply set the total number of time steps to three. The comparison of results is presented in Figure 4.

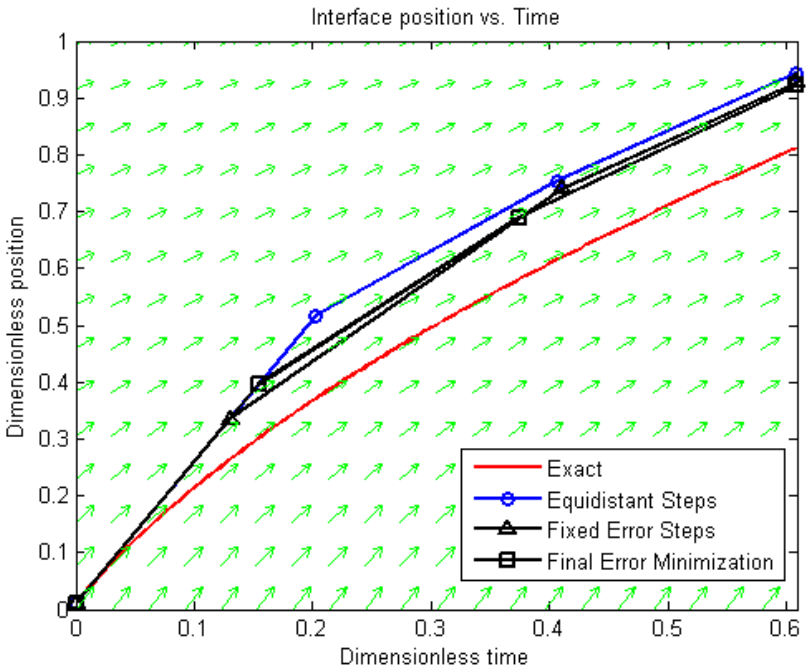

Figure 4. Comparison of the exact solution of Problem 1 with its sequential solutions: The one with equidistant time steps, the one using time steps from the fixed error time steps procedure of Section 3.1, and the one using time steps from the final error minimization procedure of Section 3.2.

The final errors (42) for the sequential method using various time steps distributions are summarized in the following table.

Time step selection procedure	*Final Error*
Equidistant Steps	18.5%
Fixed Error Steps	16.2%
Final Error Minimization	15.4%

Table 1. Final errors for sequential solutions of Problem 1 using 3 time steps.

Figure 4 shows that after the first time step the sequential solution using the fixed error steps procedure is closer to the exact solution than the one with using the final error minimization procedure. As expected, the final error minimization procedure indeed gives better results for the final error, see
Table **1**.

Consider now the solution of Problem 1 with sequential method using 10 time steps, whereas the time steps are either taken equidistant, or computed by the procedures of Sections 3.1 and 3.2. The obtained final errors are listed in the following table.

Time step selection procedure	*Final Error*
Equidistant Steps	4.26%
Fixed Error Steps	3.88%
Final Error Minimization	3.79%

Table 2. Final errors for sequential solutions of Problem 1 using 10 time steps.

The results in
Table **2** show the same qualitative behavior as in
Table **1**, although the difference between various time stepping procedures becomes smaller. As expected, the sequential method with 10 steps provides better approximation to the exact solution than the one with 3 steps. The distributions of time steps computed by the fixed error steps procedure of Section 3.1, and by the final error minimization procedure are presented in Figure 5.

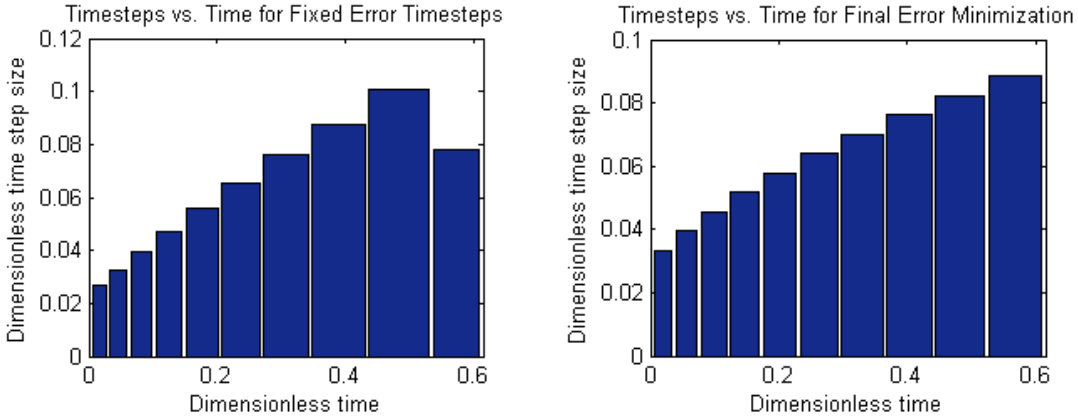

Figure 5. Distribution of time steps for the sequential solution of Problem 1 using 10 steps. Left: fixed error steps procedure. Right: final error minimization procedure.

Both sets of time steps in Figure 5 exhibit similar behaviour: At the beginning of the computation, when the exact solution has a steeper slope (cf. Figure 4), smaller time steps are required; when the solution becomes more flat at later times, larger time steps can be taken. The very last time step for the fixed error steps procedure is clipped so that the computation is stopped exactly at final time.

4. Degree of coupling of the elliptic-hyperbolic system

The results from Sections 2 and 3 can be used to give a quantitative description to the degree of coupling of the elliptic-hyperbolic IBVP (5)–(7). Indeed, as we have already noticed in Section 2, the case of the mobility ratio $M = 1$ corresponds to the situation

when the dimensionless system (28), (33) (and thus the dimensional system (5)–(7)) decouples. The exact solution for $M = 1$ is a straight line (38), so the sequential approach (41) with a single time step yields precisely this exact solution. One possible way of estimating the degree of coupling of the system (28), (33) for the cases with $M \neq 1$ is to use a difference between the exact solution and its single step approximation at certain time instant.

Let us define the *decoupling error* of the system (28), (33) as the normalized worst case error

$$E = \frac{d_{\max}}{\tilde{h}(\tilde{t}_N)}, \tag{48}$$

where $d_{\max}$ is given by (43). In Section 2 we have shown that the exact solution to the system (28), (33) can be expressed in terms of three dimensionless parameters: the mobility ratio M, the initial interface position $\tilde{h}_0$, and the parameter $\tilde{D}$, related to the shape of the Buckley–Leverett flux function. Consequently, the decoupling error is a function of three variables $E = E(M, \tilde{h}_0, \tilde{D})$.

In what follows, we analyse this functional dependence for a particular case of Problem 1 (page 12). As stated in Section 3, this problem is completely determined by the following values of dimensionless parameters: $M = 3.28$, $\tilde{h}_0 = 0.01$, and $\tilde{D} = 0.77$. The final time is set to $\tilde{T}_f = 0.61$.

In
Figure **6** we present the exact solution (37) of Problem 1 for varying values of the mobility ratio M, together with corresponding decoupling errors (48). Observe that the solution graph becomes steeper for increasing M, and the decoupling errors grow. For the almost degenerate case $M = 1.01$ the exact solution approaches the straight line (38), and the decoupling error is close to zero.

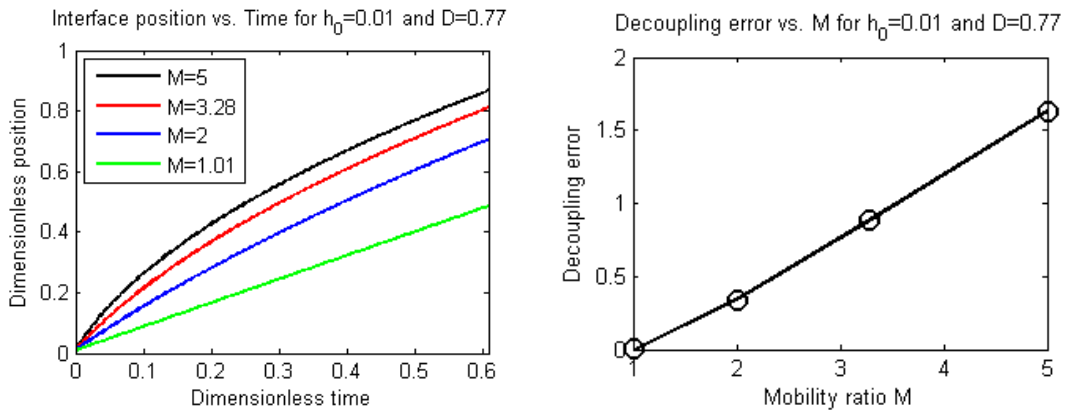

Figure 6. Left: Interface position vs. Time for Problem 1 with varying mobility ratio M. Right: corresponding decoupling errors.

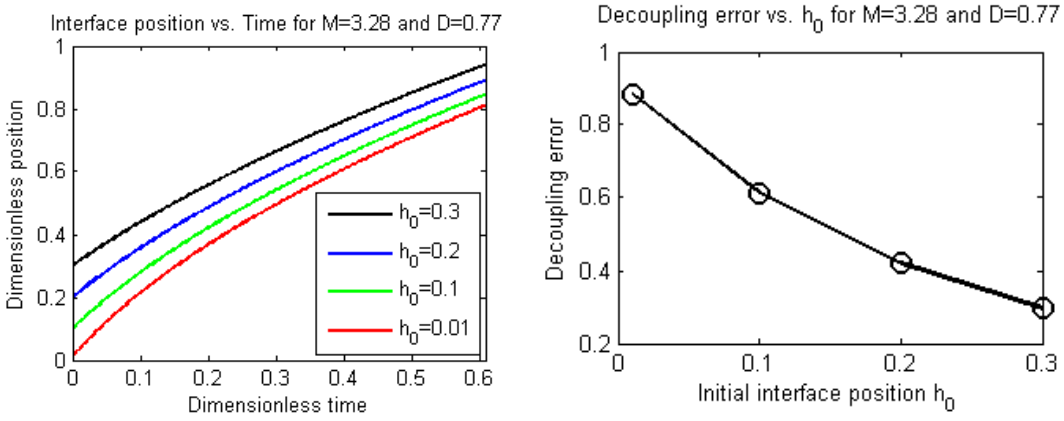

Figure 7. Left: Interface position vs. Time for Problem 1 with varying initial interface position $\tilde{h}_0$. Right: corresponding decoupling errors.

Figure 7 illustrates the dependence of the exact solution of Problem 1 on a change in the initial interface position $\tilde{h}_0$, and the corresponding decoupling errors. The graphs in Figure 7 (left) become more flat with as $\tilde{h}_0$ increases, which result in smaller decoupling errors in
Figure 7 (right).

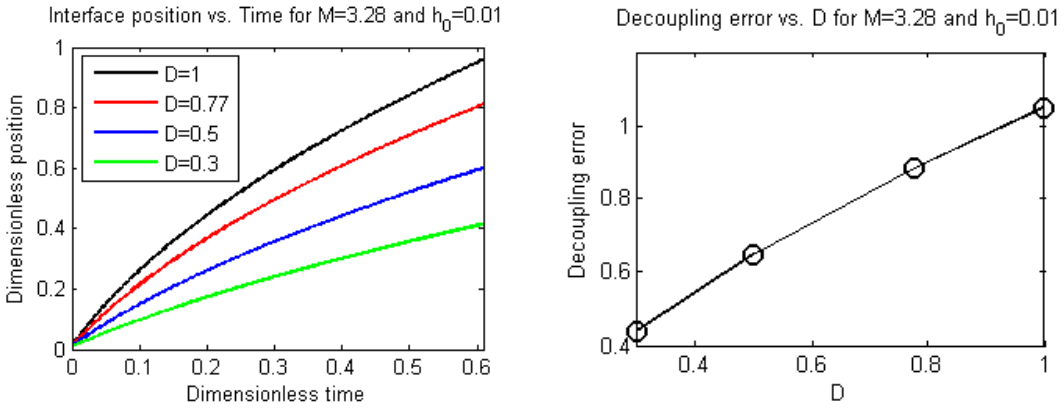

Figure 8. Left: Interface position vs. Time for Problem 1 with varying parameter $\tilde{D}$. Right: corresponding decoupling errors.

Finally, in
Figure 8 we present the exact solution of Problem 1 for varying values of the parameter $\tilde{D}$, and the corresponding decoupling errors. The graphs in

Figure **8** show qualitatively the same behaviour as the graphs for the case of varying M .

5. Conclusions and outlook

In this work, we address the issue of an optimal choice of time steps during a sequential solution of an elliptic-hyperbolic system of partial differential equations, which describes a flow of two incompressible phases in porous media. To this goal, we consider a one-dimensional version of this system, augmented with special initial and boundary conditions, in Cartesian geometry, and cylindrically and spherically symmetrical cases. For the resulting one-dimensional initial boundary value problem (IBVP), we provide an analytical solution and study its admissibility conditions. Furthermore, we show that the solution for the case of Cartesian geometry is completely determined by three dimensionless parameters: The mobility ratio, the initial position of the interface between two phases, and a parameter related to a shape of the Buckley–Leverett flux function.

The sequential solution of the one-dimensional IBVP is precisely the forward Euler method for the numerical solution of ordinary differential equations. We propose two procedures for an optimal time step selection, and test them on a sample problem for an interface motion. We show that the resulting time steps distribution yields a lower error at the end of the computation than the one obtained with equidistant time steps.
Finally, we propose to estimate the degree of coupling of the one-dimensional elliptic-hyperbolic IBVP using a normalized difference of the exact solution and a single-step sequential solution. We illustrate the change in the decoupling error by varying the determining dimensionless parameters of a sample problem for an interface motion.
This work is a first step towards an efficient time stepping selection for the sequential solution of the system of equations for multiphase flows in porous media. Practically important problems are inherently three-dimensional and heterogeneous, so the direct application of a priori estimates based on analytical one-dimensional models seems to yield only a rough guideline for the time step selection. Nevertheless, we believe that understanding of the solution on model problems and analysis of the decoupling error of the system of governing equations is an important prerequisite for an efficient solution of real-world problems.

References

1. K. Aziz and A. Settari, "*Petroleum reservoir simulation*", Applied Science Publishers Ltd, London, 1979.
2. Z. Chen, G. Huan, and Y. Ma, "Computational methods for multiphase flows in porous media", SIAM, Philadelphia, 2006.
3. A. Datta-Gupta and M. J. King, "*Streamline simulation: theory and practice*", SPE Textbook vol. 11, 2007.
4. K.H. Coats, "A note on Impes and some Impes-based simulation models", *SPE 49774*, 1999.
5. R. E. Ewing, ed., "The mathematics of reservoir simulation", *Frontiers in Applied Mathematics 1*, SIAM, Philadelphia, 1984.

6. R. E. Ewing and T. F. Russell, “Efficient time-stepping methods for miscible displacement problems in porous media”, *SIAM J. Numer. Anal.* **19** (1982) 1–66.
7. O. Ichiro, A. Datta-Gupta, and M. J. King, “Timestep selection during streamline simulation via transverse flux correction”, *SPE Journal*, **9** (2004) 459–464.
8. M. Muskat, “*The flow of homogeneous fluids through porous media*”, Edwards Inc., Ann Arbor, 1946.
9. J. C. Lagarias, J. A. Reeds, M. H. Wright, and P. E. Wright, “Convergence properties of the Nelder–Mead simplex method in low dimensions”, *SIAM J. Optimiz*. **9** (1998) 112–147.
10. C. M. Dafermos, “*Hyperbolic conservation laws in continuum physics*”, Springer, Berlin, 2000.
11. J. Bear, “*Dynamics of fluids in porous media*”, Dover, New York, 1988.
12. J. Stoer and R. Bulirsch, “*Introduction to numerical analysis*”, Springer, New York, 1993.